



Flow Characteristics on Carotid Artery Bifurcation of Different Aneurysmal Morphology

Ommar Mykael Mat Saufi¹, Nur Amani Hanis Roseman¹, Ishkrizat Taib^{1,*}, Nurul Fitriah Nasir¹, Ahmad Mubarak Tajul Ariffin¹, Nor Adrian Nor Salim¹, Shahrul Azmir Osman¹, Nofrizal Idris Darlis², Ali Kamil Kareem³

¹ Faculty of Mechanical and Manufacturing Engineering, Universiti Tun Hussein Onn Malaysia, Parit Raja, 86400 Batu Pahat, Johor, Malaysia

² Faculty of Technology, Universiti Tun Hussein Onn Malaysia, Parit Raja, 86400 Batu Pahat, Johor, Malaysia

³ Department of Biomedical Engineering, Al-Mustaqbal University College, Babylon, Iraq

ARTICLE INFO

Article history:

Received 11 August 2022

Received in revised form 12 September 2022

Accepted 10 October 2022

Available online 1 February 2023

Keywords:

Hemodynamic; carotid artery; intracranial aneurysm; CFD; blood viscosity model; velocity; wall shear stress

ABSTRACT

Aneurysm is a vascular disorder characterized by abnormal focal dilation of an artery which is considered as a serious and potentially life-threatening condition. An estimated 2%–5% of the general population is affected by intracranial aneurysms. Through computational fluid dynamic (CFD) investigation, this study aims to learn the flow characteristic on aneurysm afflicted common carotid artery (CCA). This study focused on the velocity, wall shear stress (WSS) and sensitivity of blood viscosity of the CCA flow. CFD method was done to 3 simplified model of CCA which were normal, saccular aneurysm, fusiform aneurysm CCA model. The simulation was done with different blood viscosity model which were Newtonian and non-Newtonian. The high velocity area of blood flow has corresponding effect to the increase of the WSS distribution to the wall of the geometry. The results also showed at certain value of low velocity area, WSS distribution for different blood viscosity model was deviated significantly.

1. Introduction

Aneurysm is a vascular disease characterized by local dilatation of arterial walls. It also refers to a weakening of an artery wall that creates a bulge, or distention of the artery. Most aneurysms do not show symptoms and are not dangerous. However, at their most severe stage, some can rupture, leading to life-threatening internal bleeding [1, 17, 20]. Cerebral aneurysms can cause lethal subarachnoid hemorrhage and occur more frequently in the internal carotid artery (ICA) [2]. Cerebral artery aneurysms can be divided into those that are intracranial and extracranial. Extracranial carotid artery aneurysms are rare, with an incidence of 0.5–1% accounting for less than 1% of all peripheral artery aneurysms [3]. In relation with other previous study showed the prevalence of intracranial aneurysms in the general population is approximately 2–3% [4]. Aneurysms are frequently observed

* Corresponding author.

E-mail address: iszat@uthm.edu.my (Ishkrizat Taib)

in the intracranial space and exhibit fusiform or saccular shapes [5]. The most serious complication of aneurysms is their rupture and the resulting intracranial hemorrhage into the subarachnoid space, which is associated with a high mortality and morbidity rate [4]. An estimated 2%–5% of the general population is affected by intracranial aneurysms [6].

Intracranial aneurysms are balloon-like pathologic dilations of the cerebral blood vessel walls [6]. There are 3 typical morphologic cerebral aneurysms which is saccular aneurysm, fusiform aneurysm and dissecting aneurysm. Saccular aneurysm also known as berry aneurysm has a round-like sac containing blood. It resembles a berry hanging from its branch. Based on one of the previous study, saccular aneurysm being the most common aneurysm in cerebral aneurysm (about 90% of all aneurysms) [7]. A fusiform aneurysm has a balloons or bulges shape that extrudes out on all sides of the artery. Fusiform aneurysm is common occurs in internal carotid artery distribution [8, 19]. Figure 1 showed an image of both saccular and fusiform aneurysms. Dissecting aneurysm is a separation of the artery wall layer that causes tear in the artery wall, rather than bulging out like fusiform aneurysm. This is the least common aneurysm compared between the other two as one previous study suggest; It is extremely rare for aneurysms to develop secondary to dissection of the intracranial arteries as publications concerning dissecting aneurysms of the intracranial carotid circulation have been limited to case reports [9].

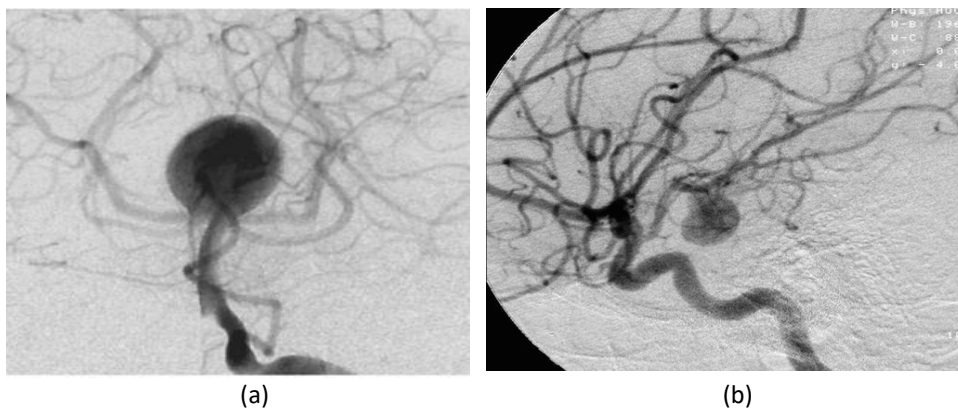


Fig. 1. Digital subtraction angiography image of intracranial (a) fusiform aneurysm (b) saccular aneurysm [7].

Many efforts in research has been done to study the development of rupture to predict aneurysm rupture. The study on the development of aneurysm helped in distinguishing high-risk aneurysm to rupture for immediate treatment. Prediction of aneurysm is difficult, complex, time consuming and costly [10]. Therefore, researchers have applied CFD simulation to gain better insights of the intra-aneurysmal hemodynamics [2, 18, 21, 23]. Using computational fluid dynamics (CFD) simulation to achieve better insight of hemodynamic parameters have been reported to be valuable predictors for aneurysmal rupture [10]. Hemodynamic studied the blood flow and presented as the principles that control the distribution of blood flow and blood pressure in the vascular system [12, 24]. It is important to consider hemodynamic in studying flow characteristic on aneurysm as hemodynamic factors, including wall shear stress (WSS) is known as a risk indicator for aneurysm development and rupture [11]

Other than that, the geometric structure and mechanical properties of the remodeled vessel also play a major role in disease process including aneurysm [12]. This is because the direction that blood flows once an aneurysm form depends on aspects such as neck diameter, its angle with respect to the parent artery, or the angle of efferent vessels, and aneurysm morphology [4]. In hemodynamic of arterial flow, the WSS is presented as the force per unit area exerted by the wall on the fluid in a

direction on the local tangent plane [13]. It is shown that a normal artery needed a specific level of WSS to have normal functioning. In the contrary, low and high WSS distribution to aneurysm region might differ from that to a healthy artery as the progression and rupture of aneurysms have been correlated with region of the aneurysm wall exposed to both high and low WSS [4].

A complete description of hemodynamics within the carotid artery requires knowledge of the pattern of blood velocities within the flow. It not only depends on the geometry and mechanical properties of the artery wall but also depends to an overall pressure difference, and the rheological characteristics of blood such as viscosity and density [14]. Knowledge of this set of parameters at the artery wall allows evaluation of WSS values and thus may provide indications for estimating the risk for development and progression of aneurysm and hemorrhage associated with cerebral aneurysms [14, 22].

The purpose of this study is to use CFD simulation on a simplified model to analyze the flow characteristic in an aneurysm artery. The use of CFD enable the application of variety parameters in hemodynamic to determine the factor that contribute to the rupture of aneurysm. The hemodynamic parameter that was focused on in this study was WSS. CFD simulation was done on 3 simplified models included a normal carotid artery, fusiform aneurysm inflicted carotid artery and saccular aneurysm inflicted carotid artery. The simulation was also done with different blood viscosity model; Newtonian and non-Newtonian (Carreau-Yasuda model).

2. Methodology

2.1 Carotid Artery Simplified Model Geometry

Several models from the previous study [2, 6, 11, 14] are reviewed to have better insights on the geometry properties of an average carotid artery. The simplified models were designed using CAD software. The first design of the simplified model is a healthy common carotid artery with no bulges. The model was designed with 7.4 mm CCA inlet, 5.0 mm internal carotid artery (ICA) inlet and 4.4 mm external carotid artery (ECA) inlet. The second model designed of saccular aneurysm afflicted CCA with 7 mm aneurysm sac. The third model constructed was a fusiform type of aneurysm afflicted CCA with 9.7 mm aneurysm sac. The three models are shown in Figure 2 below.

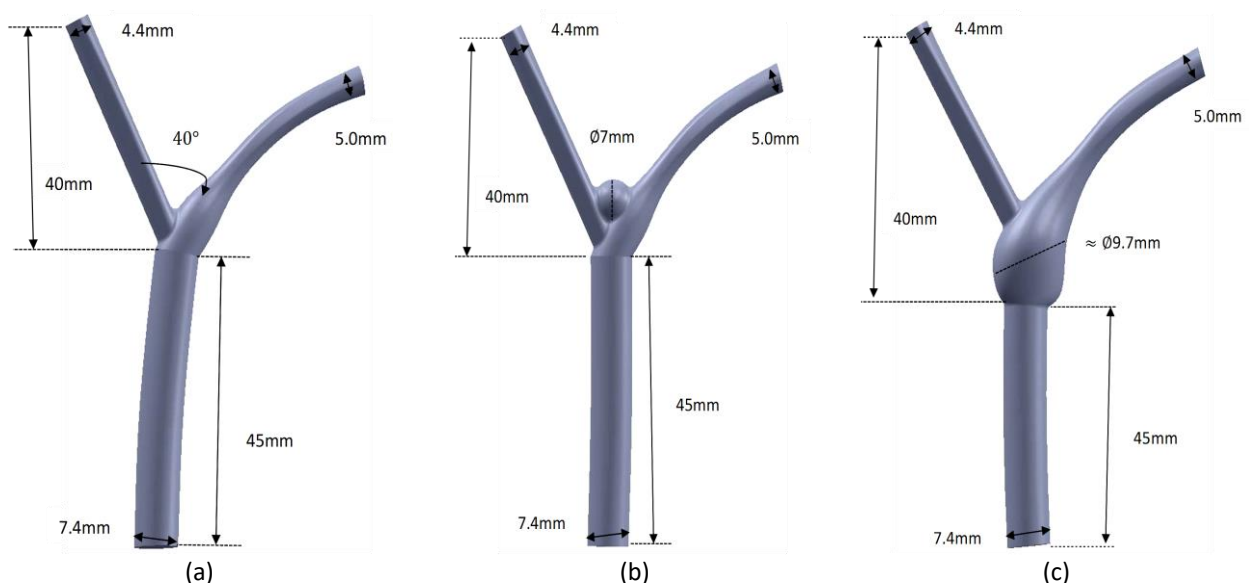


Fig. 2. a) Simplified model of CCA b) Simplified model of CCA with saccular type aneurysm c) Simplified model of CCA with fusiform type aneurysm.

2.2 Parameter Assumptions and Boundary Conditions

The fluid flow was assumed incompressible, homogenous and the type of flow used was transient flow. Vessel walls were assumed rigid and no slip boundary conditions were applied. Distal vascular beds were assumed to have similar total resistance to flow, traction-free boundary conditions with the same pressure level were applied to all model outlets. The velocity gradient was assumed zero at the outlet. At the inlet for all models, velocity profile was defined as laminar and described as fully developed velocity profile. For the blood flow velocity, a realistic transient inlet velocity model is used which for a sine wave of a maximum velocity of 0.5 m/s, the period of each cycle is 0.5 seconds and the simulation is done for one cycle. Figure 3 showed the average inlet velocity boundary condition as it varies with time during a period of 0.5 second (which represents a pulse rate of 120 pulse/minute). The velocity inlet is inserted to Fluent as a user defined function and the code used, written by Chiyu Jiang from Cornell University [15]. Table 1 showed the summary of parameter and boundary condition used for the simulation setup in Ansys Fluent.

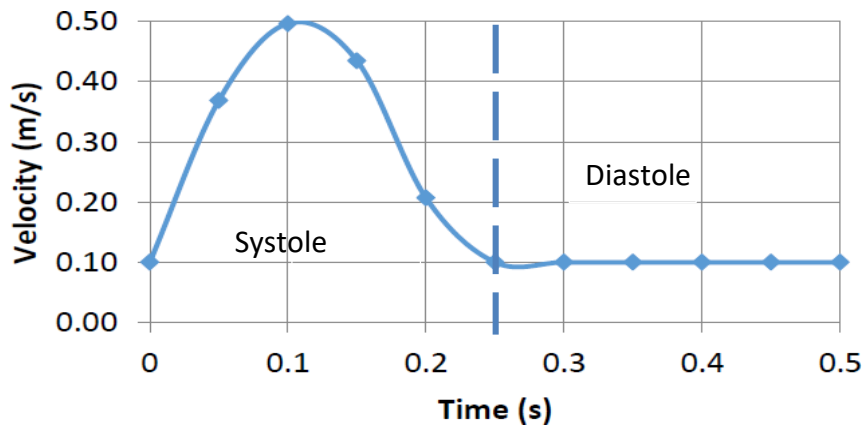


Fig. 3. UDF Inlet velocity profile written by Chiyu Jian [15]

Table 1

Boundary conditions and Parameters Configuration for Simulation

Density	$\rho=1060 \text{ kg/m}^3$	
Inflow rate profile	Fully Develop Laminar Flow	
Outflow vessel blood pressure	$p = 100\text{mmHg}$ or 13332Pa	
Inflow blood velocity	$v = 0.1\text{-}0.5\text{m/s}$ (pulsatile flow)	
Arterial Wall	No slip and Rigid	
Model	k-omega (for Newtonian setup) laminar (for non-Newtonian setup)	
Solution of Pressure- Velocity Coupling	SIMPLE (default setting)	
Blood Viscosity Model	Newtonian Blood model	Constant blood viscosity $=0.0035 \text{ Pa}\cdot\text{s}$
	Non-Newtonian Blood model (Carreau-Yasuda)	zero shear rate viscosity= $0.056 \text{ Pa}\cdot\text{s}$ infinite shear rate viscosity= $0.0035 \text{ Pa}\cdot\text{s}$ Time constant= 3.313s Power Law Index = 0.3568

2.3 Governing Equation

The velocity of inlet and pressure outlet was computed in ANSYS Fluent to solve the continuity and Navier-Stokes equation. Blood flow is treated mathematically as an incompressible Newtonian fluid. The governing equations are the time-dependent Navier-Stokes equations, which express the conservation of linear momentum:

$$\rho \left(\frac{\partial \vec{v}}{\partial t} + \vec{V} \cdot \nabla \vec{V} \right) = -\nabla \cdot \tau - \nabla p \quad (1)$$

These equations are subjected to the incompressibility condition, which expresses the conservation of mass:

$$\nabla V = 0 \quad (2)$$

The shear stress, WSS at wall of aneurysm is calculate based on a function of velocity gradient only:

$$WSS = \mu \frac{\partial u}{\partial y} \quad (3)$$

WSS is defined in a Cartesian coordinate system as μ is the viscosity u , v and w are the velocity components in x , y and z respectively. In the simulations carried out here, the magnitude and direction of each scalar is determined at every wall grid point.

$$WSS = \mu \left(\frac{\partial u}{\partial x} + \frac{\partial v}{\partial y} + \frac{\partial w}{\partial z} \right) \quad (4)$$

3. Results and Discussion

3.1 Grid Independence Test (GIT)

GIT method was done to select the best mesh setup for the simulation in terms of low average error of velocity and for best time management. The mesh setup was done multiple times with the increment of 50,000 number nodes approximately. A set of data was taken from each of the mesh setup as shown in Figure 4. Eq. (5) was used to calculate the relative error percentage the meshes setup and the relative error of average velocity along the bifurcation to the ICA was calculated using Eq. (6). The result was tabulated in Table 2. For this simulation, the 153k node is chosen because it has the lowest error percentage and skewness.

$$\text{Percentage Error} = \frac{\text{Latest mesh} - \text{previous mesh}}{\text{Latest mesh}} \times 100 \quad (5)$$

$$\text{Velocity Average} = \sum \left(\frac{\text{velocity along the bifurcation to the ICA}}{\text{Number of sample}} \right) \quad (6)$$

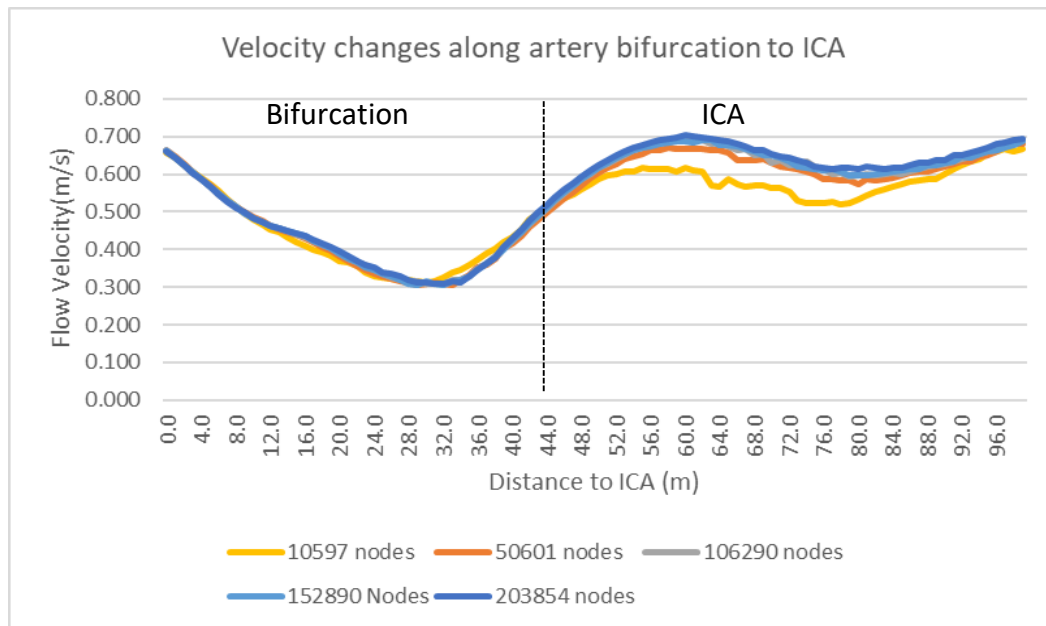


Fig. 4. Velocity changes along artery bifurcation to ICA for different meshing.

Table 2

Result of velocity average error at bulging area

GIT	Numberof nodes	Number of elements	Max skewness	Relative error percentage ofaverage velocity along the bifurcation to ICA (%)
1	10 597	518 49	0.8456	-
2	69 918	268 997	0.8432	3.832
3	107 568	582 160	0.8492	1.637
4	153 467	835 369	0.8332	0.1286
5	212 688	1 130 415	0.8486	1.1438

3.2 Comparison of Simulation Study

The maximum velocity of blood flow from this study is compared and verified using the model design of a simplified model of a carotid artery based on MRI of 5 patients by Mhd and Alargha [15] in Figure 5. The boundary condition and parameter are similar by way of the arterial wall was set as rigid and no slip boundary. The design model used is the blood viscosity model of Carreau-Yasuda. The result of simulation produces a relative error value below the acceptable value of 10% as shown in Table 3.

Antonova *et al.*,
 [16].
 Velocity
 SimulationResult

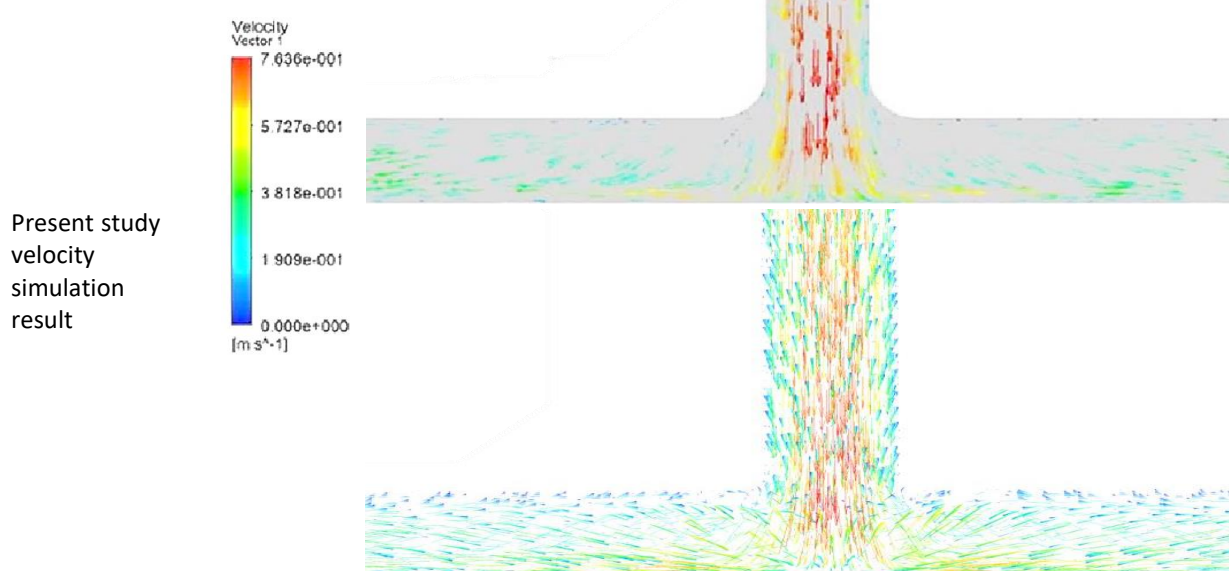


Fig. 5. Velocity of blood flow between previous research study model and present study model

Table 3

Comparison between previous study model and present model

CCA ModelDesign	Element size (m)	Number of Elements	Maximum Blood Flow Velocity (m/s)	Relative Percentage Error
(Mhd and Alargha, 2016)	0.008	144,000	0.764	
Present Study	0.005	174,496	0.727	4.84%

3.3 Viscosity Sensitivity Study on Velocity and WSS Analysis

Viscosity sensitivity study is conducted to compare between the application of Newtonian and non-Newtonian (Carreau-Yasuda) blood model by simulate 3 models of different morphology of simplify CCA (healthy CCA, saccular aneurysm afflicted CCA and fusiform afflicted CCA). The models were compare based on the variation of velocity streamlines of the model blood flow and the WSS.

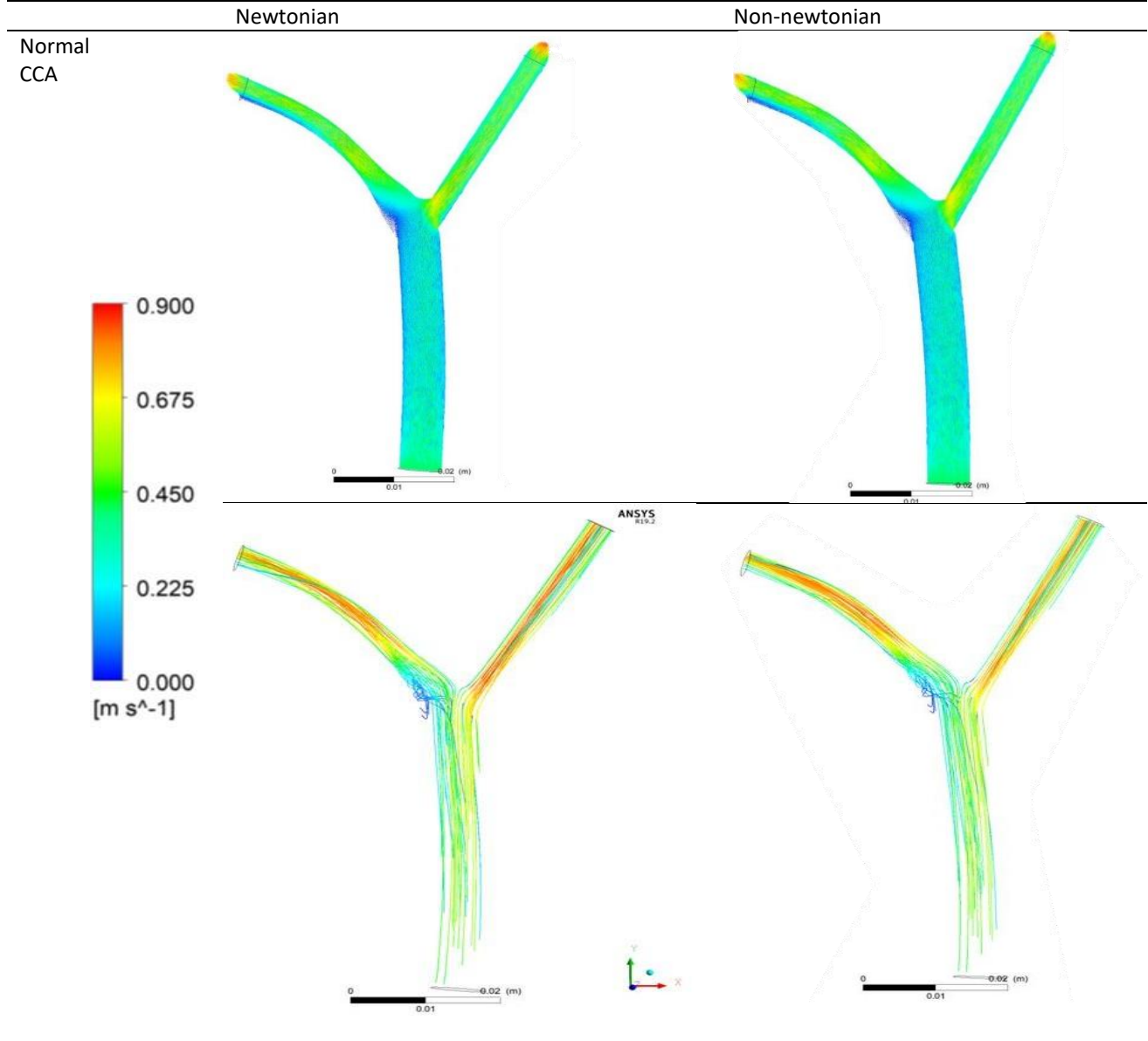
3.3.1 Velocity analysis

The three simplified carotid models showed a relatively similar pattern when comparing between the Carreau-Yasuda and the Newtonian viscosity models for velocity. In these figures, the reddish colour represents the highest value for velocity and bluish colour represents the lowest values of velocity. The simulation was taken at 0.1 second (systole) for all model.

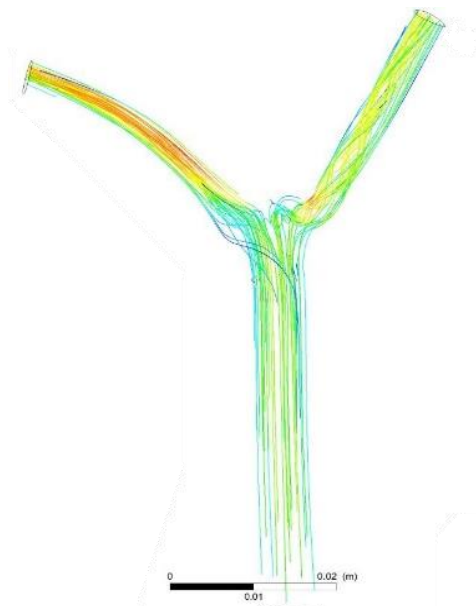
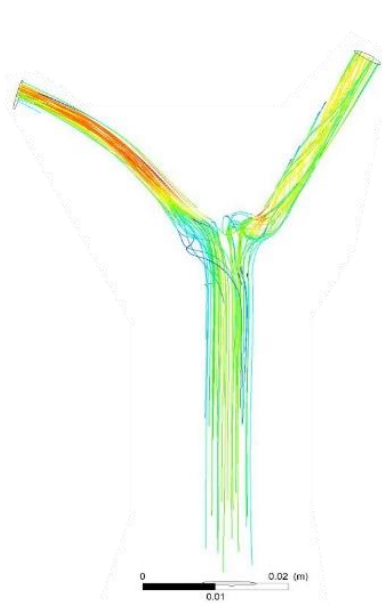
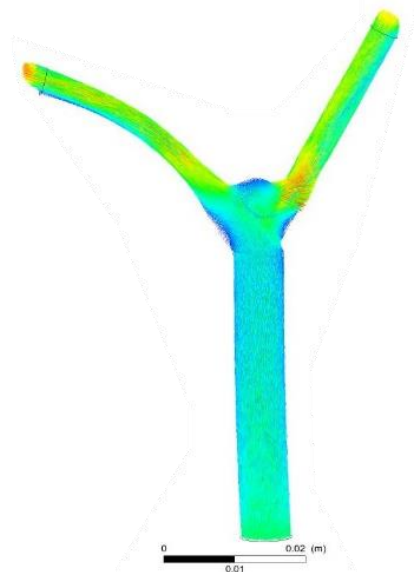
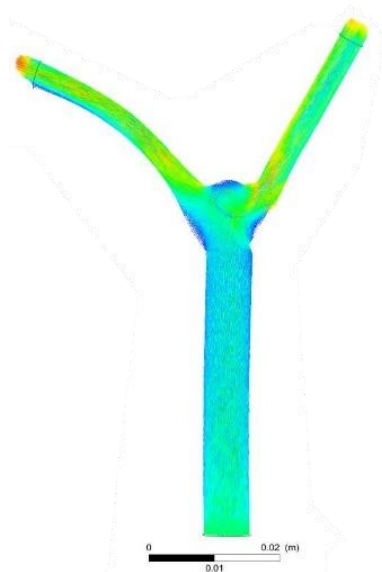
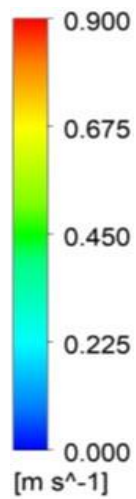
Shown in Table 4 that slow velocity flow occurred at the ICA entrance and high velocity appeared high at the end of each daughter artery. This is because due to the geometry of the neck size of the artery. Large neck size made large flow area caused slow velocity whereas small neck size caused

high velocity. Both the saccular and fusiform aneurysm dome exhibited slow velocity flow allowed blood near zero velocities at the aneurysmal flow which caused weak swirl.

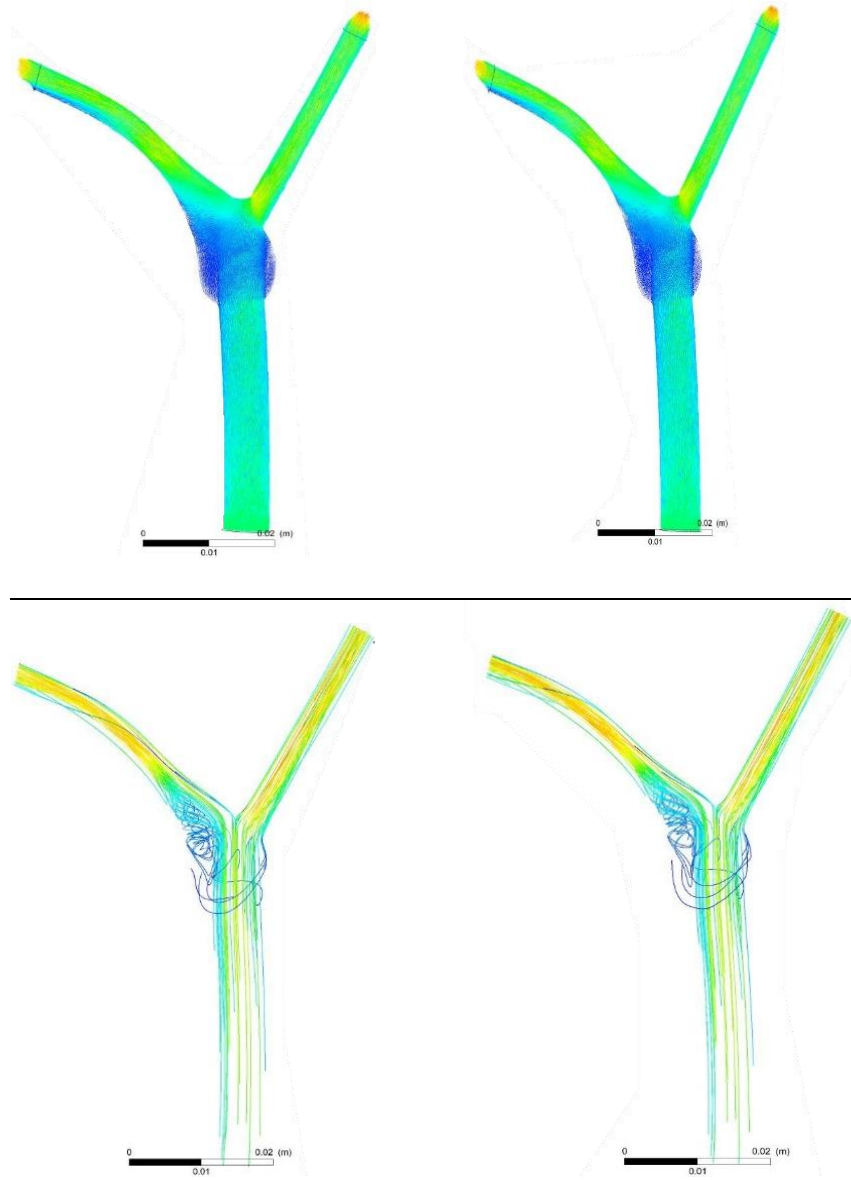
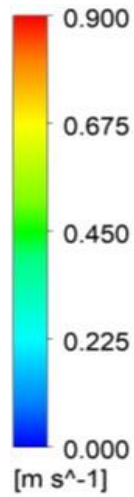
Table 4
Velocity of normal CCA, saccular and fusiform afflicted CCA in different blood models



Saccular
aneurysm
m CCA



Fusiform
aneurysm CCA



3.3.2 WSS analysis

Table 5 shows a comparison of saccular aneurysm and fusiform aneurysm was distribution to the arterial wall for Newtonian and Non-Newtonian blood viscosity model. This WSS is taken at 0.1 second (systole) as to have the highest value of velocity intake which is $v=0.5$ m/s. It can be seen that correspond to the velocity figure showed high velocity produces high WSS distribution to the wall. The different WSS distribution from both viscosity was visible at the low velocity bifurcation area. For saccular aneurysm the different behavior of WSS from different blood viscosity can be seen around the saccular dome area. The low distribution of WSS around aneurysmal wall was as expected because blood vessel developed aneurysm to decrease the shear force exerted on the wall thus lowering the WSS distribution.

Table 5
 WSS of aneurysm afflicted CCA on different blood models

Aneurysm	Newtonian	Non-Newtonian
Saccular		
Fusiform		

3.4 Viscosity Simulation

The normalized WSS (minimum value, maximum value and average value) was calculated for blood viscosity models to show the deviation between them. The normalized on the normal CCA model geometry. The calculation was done on two timesteps (0.1 sec and 0.3 sec) and at two locations; the bifurcation area to the ICA and at the main CCA artery as shown in Figure 6 to Figure 9.

Based on Figures 7 and 8, the deviation data show a true minor deviation for maximum WSS and area average for bifurcation area at 0.1 second. At 0.3 seconds timestep. For Figure 8 and 9, at timestep 0.1 seconds also showed another minor deviation that support the evidence from the data collected from the bifurcation but in a lower pattern of changes. This is because the area of sampling has good increment of WSS distribution so the result obtained have higher accuracy than that at the

bifurcation area. At 0.3 seconds timestep, the deviation was significant and this is because the large difference between the two viscosity models always occurs at the minimum WSS bar because it occurs at minimum speed hence minimum strain rate and maximum effective viscosity difference. At the CCA artery, it is noticed that WSS for the models are relatively the same due to the high magnitude of velocities at area at time step 0.1 second.

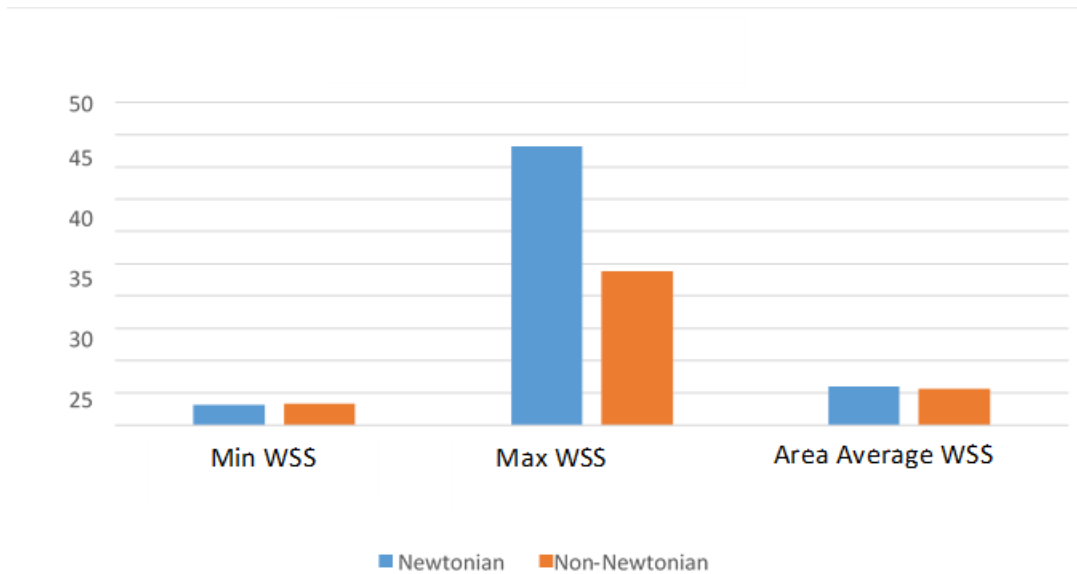


Fig. 6. Normalized WSS at bifurcation to ICA for different viscosity model at 0.1

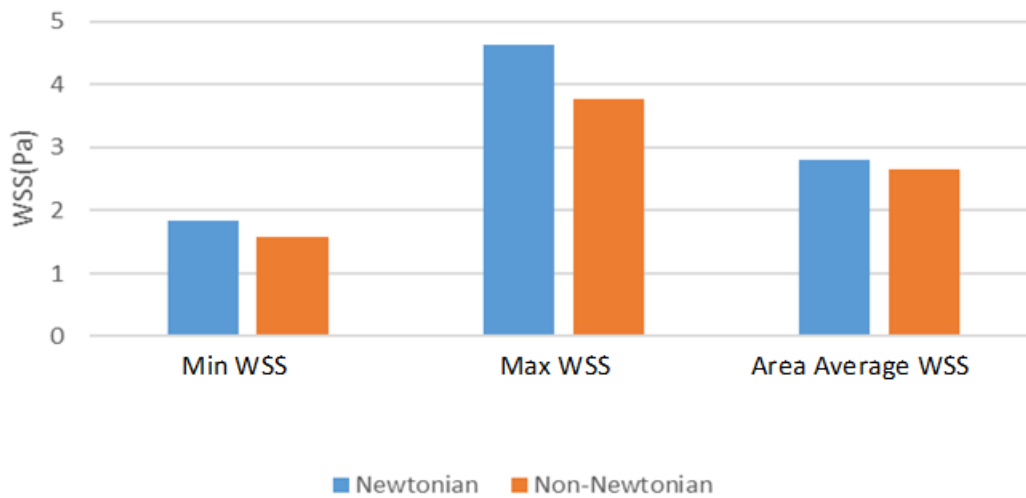


Fig. 7. Normalized WSS at bifurcation to ICA for different viscosity model at 0.3

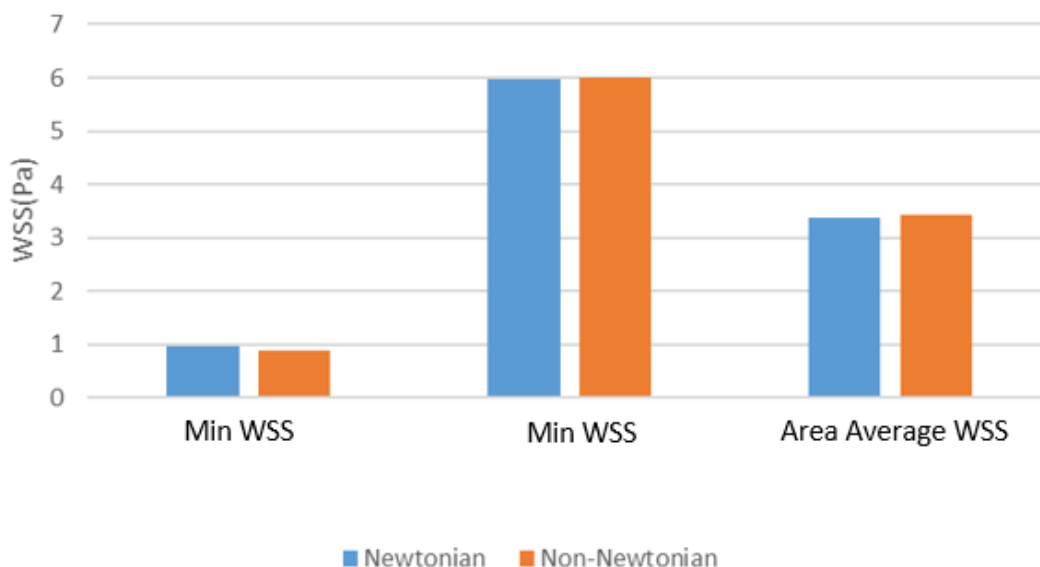


Fig. 8. Normalized WSS at CCA for different viscosity model at 0.1 second

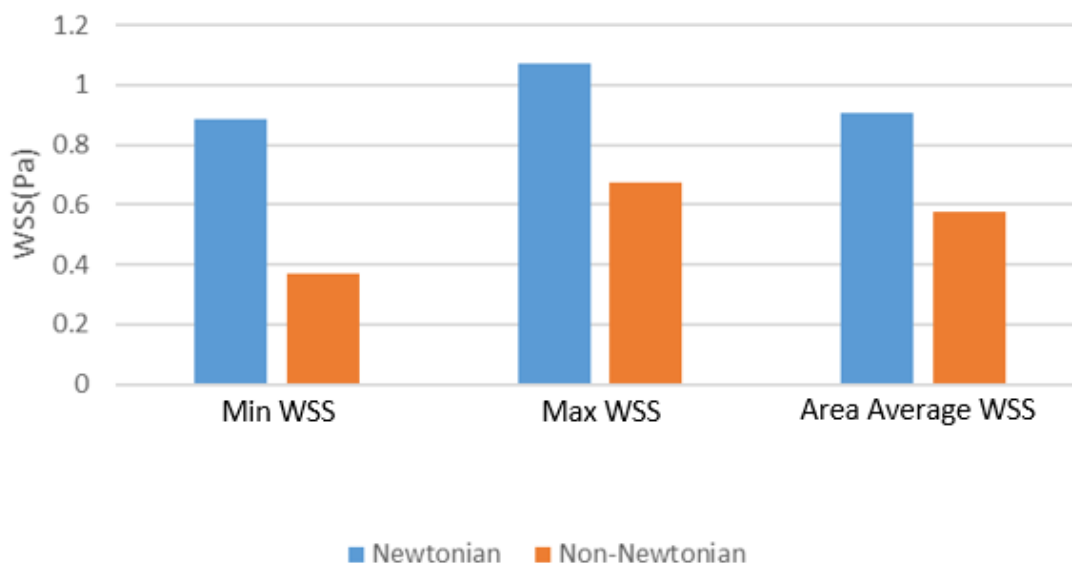


Fig. 9. Normalized WSS at CCA for different viscosity model at 0.1 second

From Figure 10, deviation was at the lowest when the max WSS was obtained during the systole. This was due to high velocity during systole cause low deviation. Conversely at 0.3 second where the cycle entered diastole, WSS was at the lowest corresponding with the low velocity flow. This caused the deviation to increase significantly as showed in the graph the deviation reached its peak value of 32% which was relatively too high for simulation standard. In conclusion, based on the result obtained from the graph, the Newtonian model can be used to predict WSS at high blood velocity (0.5 m/s) while for low velocity (>0.1 m/s) non-Newtonian model should be used as Newtonian will obfuscate the WSS result.

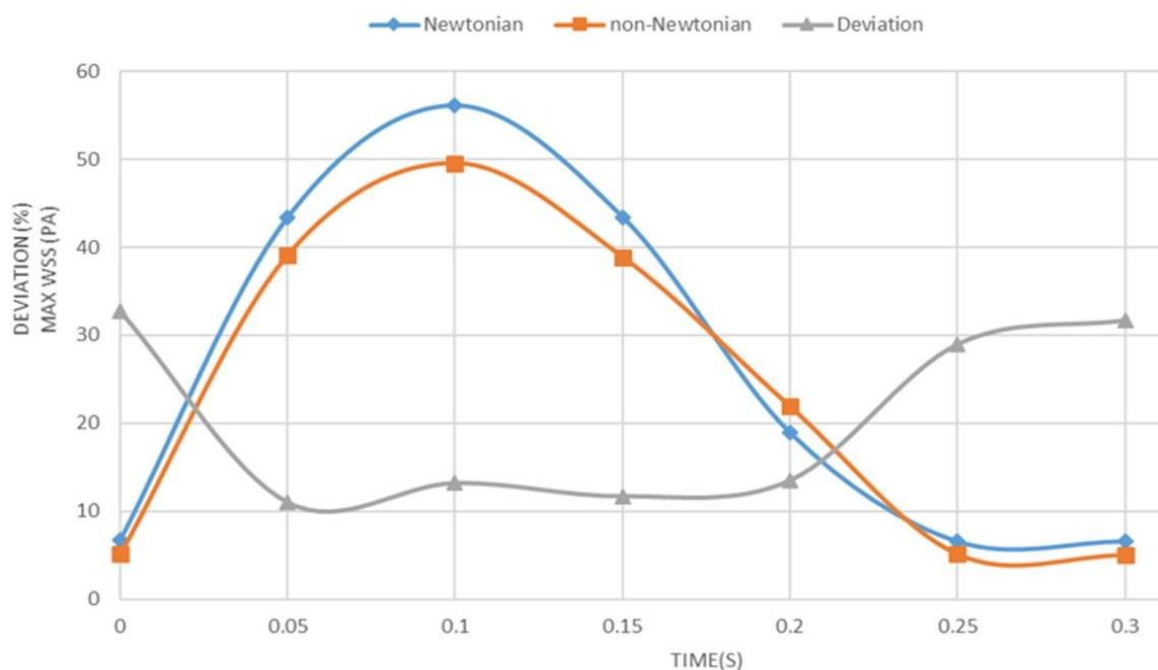


Fig. 10. Graph of Max WSS against time

4. Conclusion

The result obtained from the simulation showed that the flow characteristic such as velocity and WSS was dependent on the geometry of the model being simulated. The result gave evidence that the small size of the neck for the blood flow entrance caused the velocity of blood flow to increase while a large neck size caused slower speed such as in the aneurysm dome. It was also founded that the elevation of the velocity of blood flow was corresponded to the increase of the WSS distribution. The result also confirmed that blood vessel developed aneurysm to decrease the shear force exerted to the arterial wall thus decreasing the WSS distribution around the aneurysmal wall. The result obtained from the simulation done for two types of blood viscosity models which were Newtonian and non-Newtonian succeeded in determining the effect of blood viscosity on the flow characteristic of carotid artery. It was found that deviation of blood viscosity was high at a low-velocity area of blood flow. Therefore, the application of Newtonian fluid for flow with the velocity that was below 0.1 m/s was not suitable as it will under predict the WSS.

Acknowledgement

This research has been supported by the Ministry of Higher Education (MOHE) through the Fundamental Research Grant Scheme (FRGS) (FRGS/1/2020/TK0/UTHM/03/38)

References

- [1] Hong, Lim Sheh, Mohd Azrul Hisham Mohd Adib, Muhammad Uzair Matalif, Mohd Shafie Abdullah, Nur Hartini Mohd Taib, and Radhiana Hassan. "Modeling and simulation of blood flow analysis on simplified aneurysm models." In *IOP Conference Series: Materials Science and Engineering*, vol. 917, no. 1, p. 012067. IOP Publishing, 2020. <https://doi.org/10.1088/1757-899X/917/1/012067>
- [2] Castro, M. A., Christopher M. Putman, and J. R. Cebral. "Computational fluid dynamics modeling of intracranial aneurysms: effects of parent artery segmentation on intra-aneurysmal hemodynamics." *American Journal of Neuroradiology* 27, no. 8 (2006): 1703-1709.
- [3] Davey, P. T., I. Rychlik, M. O'Donnell, R. Baker, and I. Rennie. "An internal carotid artery aneurysm presenting with dysarthria." *The Annals of The Royal College of Surgeons of England* 95, no. 7 (2013): e6-e8. <https://doi.org/10.1308/003588413X13629960047713>

- [4] Munarriz, Pablo M., Pedro A. Gómez, Igor Paredes, Ana M. Castaño-Leon, Santiago Cepeda, and Alfonso Lagares. "Basic principles of hemodynamics and cerebral aneurysms." *World neurosurgery* 88 (2016): 311-319. <https://doi.org/10.1016/j.wneu.2016.01.031>
- [5] Jeong, Woowon, and Kyehan Rhee. "Hemodynamics of cerebral aneurysms: computational analyses of aneurysm progress and treatment." *Computational and mathematical methods in medicine* 2012 (2012). <https://doi.org/10.1155/2012/782801>
- [6] Li, W., and Y. Wang. "Regarding "Differences in Hemodynamics and Rupture Rate of Aneurysms at the Bifurcation of the Basilar and Internal Carotid Arteries"." *American Journal of Neuroradiology* 38, no. 8 (2017): E51-E51. <https://doi.org/10.3174/ajnr.A5224>
- [7] Toth, Gabor, and Russell Cerejo. "Intracranial aneurysms: Review of current science and management." *Vascular Medicine* 23, no. 3 (2018): 276-288. <https://doi.org/10.1177/1358863X18754693>
- [8] Shokunbi, M. Tayo, H. V. Vinters, and J. C. E. Kaufmann. "Fusiform intracranial aneurysms. Clinicopathologic features." *Surgical neurology* 29, no. 4 (1988): 263-270. [https://doi.org/10.1016/0090-3019\(88\)90157-7](https://doi.org/10.1016/0090-3019(88)90157-7)
- [9] Chuang, Ming-Jung, Cheng-Hsien Lu, and Min-Hsiung Cheng. "Management of middle cerebral artery dissecting aneurysm." *Asian Journal of Surgery* 35, no. 1 (2012): 42-48. <https://doi.org/10.1016/j.asjsur.2012.04.007>
- [10] Murayama, Yuichi, Soichiro Fujimura, Tomoaki Suzuki, and Hiroyuki Takao. "Computational fluid dynamics as a risk assessment tool for aneurysm rupture." *Neurosurgical focus* 47, no. 1 (2019): E12. <https://doi.org/10.3171/2019.4.FOCUS19189>
- [11] Yamaguchi, Ryuhei, Taihei Kotani, Gaku Tanaka, Simon Tupin, Kahar Osman, Nadia Shaira Shafii, Ahmad Zahran Md Khudzari et al. "Effects of elasticity on wall shear stress in patient-specific aneurysm of cerebral artery." *Journal of Flow Control, Measurement & Visualization* 7, no. 02 (2019): 73. <https://doi.org/10.4236/jfcmv.2019.72006>
- [12] Secomb, T. W. "Hemodynamics. Comprehensive Physiology 6." *Compr Physiol.* 6, no. 2 (2016): 975. <https://doi.org/10.1002/cphy.c150038>
- [13] Jou, L-D., Deok Hee Lee, Hesham Morsi, and Michel E. Mawad. "Wall shear stress on ruptured and unruptured intracranial aneurysms at the internal carotid artery." *American Journal of Neuroradiology* 29, no. 9 (2008): 1761-1767. <https://doi.org/10.3174/ajnr.A1180>
- [14] Katritsis, Demosthenes, Lambros Kaiktsis, Andreas Chaniotis, John Pantos, Efstathios P. Efstathopoulos, and Vasilios Marmarelis. "Wall shear stress: theoretical considerations and methods of measurement." *Progress in cardiovascular diseases* 49, no. 5 (2007): 307-329. <https://doi.org/10.1016/j.pcad.2006.11.001>
- [15] Hicham Alargha, Hashem Mhd. "Numerical Analysis for the Hemodynamics in unruptured Cerebral Aneurysms." (2016).
- [16] Antonova, Nadia, X. Dong, P. Tosheva, Efstathios Kaliviotis, and I. Velcheva. "Numerical analysis of 3D blood flow and common carotid artery hemodynamics in the carotid artery bifurcation with stenosis." *Clinical hemorheology and microcirculation* 57, no. 2 (2014): 159-173. <https://doi.org/10.3233/CH-141827>
- [17] Algabri, Yousif A., Surapong Chatpun, and Ishkrizat Taib. "An investigation of pulsatile blood flow in an angulated neck of abdominal aortic aneurysm using computational fluid dynamics." *Journal of Advanced Research in Fluid Mechanics and Thermal Sciences* 57, no. 2 (2019): 265-274.
- [18] Basri, Adi Azriff, SM Abdul Khader, Cherian Johny, Raghuvir Pai, Mohammed Zuber, Zainuldin Ahmad, and Kamarul Arifin Ahmad. "Effect of single and double stenosed on renal arteries of abdominal aorta: A computational fluid dynamics." *CFD Letters* 12, no. 1 (2020): 87-97.
- [19] Zin, Ahmad Faiz Mat, Ishkrizat Taib, Muhammad Hanafi Asril Rajo Mantari, Bukhari Manshoor, Ahmad Mubarak Tajul Arifin, Mahmud Abd Hakim Mohamad, Muhammad Sufi Roslan, and Muhammad Rafiuddin Azman. "Temperature Variation with Hemodynamic Effect Simulation on Wall Shear Stress in Fusiform Cerebral Aneurysm." *Journal of Advanced Research in Fluid Mechanics and Thermal Sciences* 95, no. 2 (2022): 40-54. <https://doi.org/10.37934/arfmts.95.2.4054>
- [20] Shafii, Nadia Shaira, Ryuhei Yamaguchi, Ahmad Zahran Md Khudzari, Gaku Tanaka, Atsushi Saitoh, Makoto Ohta, and Kahar Osman. "Hemodynamic and Flow Recirculation Effect on Rupture Prediction of Middle Cerebral Artery Aneurysm." *Journal of Advanced Research in Fluid Mechanics and Thermal Sciences* 79, no. 1 (2020): 1-16. <https://doi.org/10.37934/arfmts.79.1.116>
- [21] Hong, Lim Sheh, Mohd Azrul Hisham Mohd Adib, Mohd Shafie Abdullah, and Radhiana Hassan. "Qualitative and Quantitative Comparison of Hemodynamics Between MRI Measurement and CFD Simulation on Patientspecific Cerebral Aneurysm—A Review." *Journal of Advanced Research in Fluid Mechanics and Thermal Sciences* 68, no. 2 (2020): 112-123. <https://doi.org/10.37934/arfmts.68.2.112123>
- [22] Miah, Md Abdul Karim, Shorab Hossain, and Sayedus Salehin. "Effects of Severity and Dominance of Viscous Force on Stenosis and Aneurysm During Pulsatile Blood Flow Using Computational Modelling." *CFD Letters* 12, no. 8 (2020): 35-54. <https://doi.org/10.37934/cfdl.12.8.3554>

- [23] Mahrous, Samar A., Nor Azwadi Che Sidik, and Khalid M. Saqr. "Newtonian and non-Newtonian CFD models of intracranial aneurysm: a review." *CFD Letters* 12, no. 1 (2020): 62-86.
- [24] Khairi, Nur Afikah, Mohd Azrul Hisham Mohd Adib, Nur Hazreen Mohd Hasni, and Mohd Shafie Abdullah. "Effect of Hemodynamic Parameters on Physiological Blood Flow through Cardiovascular Disease (CVD)–The Perspective Review." *Journal of Advanced Research in Fluid Mechanics and Thermal Sciences* 74, no. 1 (2020): 19-34. <https://doi.org/10.37934/arfmts.74.1.1934>